# Supporting Information

## Electrospun Fluorescent Sensors on Selective Detection of Nitro Explosive Vapors and Trace Water

Wandan Wu,[a] Naien Shi,*[a] Jun Zhang,[a] Xiaodong Wu,[a] Tao Wang,[a] Lei Yang,[a] Rui Yang,[a] Changjin Ou,[a] Wei Xue,[a] Xiaomiao Feng,[a] Linghai Xie[a], Wei Huang*[abc]

[a]*Key Laboratory for Organic Electronics and Information Displays & Institute of Advanced Materials (IAM), Jiangsu National Synergetic Innovation Center for Advanced Materials (SICAM), Nanjing University of Posts & Telecommunications, 9 Wenyuan Road, Nanjing, China*

[b]*Key Laboratory of Flexible Electronics (KLOFE) & Institute of Advanced Materials (IAM), Jiangsu National Synergetic Innovation Center for Advanced Materials (SICAM), Nanjing Tech University (NanjingTech), 30 South Puzhu Road, Nanjing, China*

[c]*Shanxi Institute of Flexible Electronics (SIFE), Northwestern Polytechnical University (NPU), 127 West Youyi Road, Xi'an 710072, Shanxi, China*

E-mail: iamneshi@njupt.edu.cn, wei-huang@njtech.edu.cn

## *A.* The diameter distribution of the PS/PyCz porous nanofibers

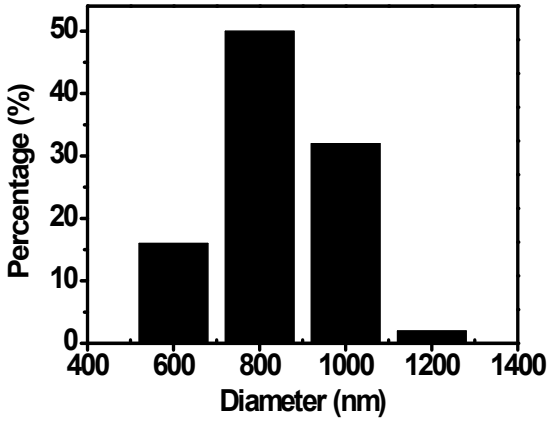


**Fig. S1** The statistical diameter distribution of PS/PyCz nanofibers shown in Fig. 1a in the text.

## *B.* TEM and distribution of porosity of the PS/PyCz porous nanofibers

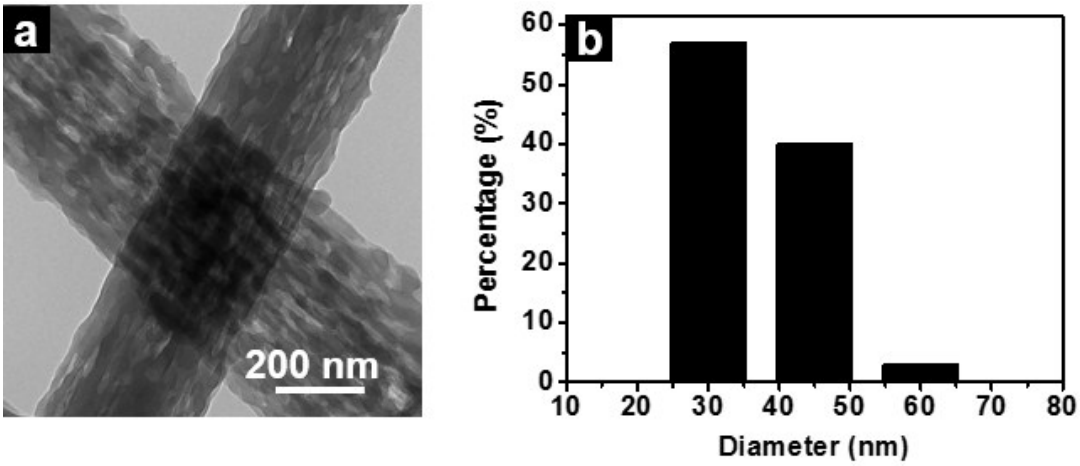


**Fig. S2** (a) TEM image of PS/PyCz porous nanofibers. (b) The corresponding statistical pore distribution of the average length of the short edge of the pores in the nanofibers.

## *C.* The calculated energy levels for different conformations of excited-state PyCz

**Table S1.** The energy levels for different conformations of PyCz and corresponding differences in the HOMO-LUMO level that decide the emissions. Geometry optimization and energy calculation are performed by time-dependent density functional theory (TD-DFT) with the basis of B3LYP/6-31G(d).

| Dihedral Angel (°) | LUMO (eV) | HOMO (eV) | $\Delta E$ $(eV)$ |
|---|---|---|---|
| 89.2[a] | -1.994 | -5.207 | 2.640 |
| 85 | -1.992 | -5.205 | 2.641 |
| 75 | -1.985 | -5.191 | 2.655 |
| 70 | -1.979 | -5.181 | 2.666 |
| 65 | -1.971 | -5.170 | 2.680 |
| 64.2[b] | -1.964 | -5.159 | 2.695 |

Notes: *a* indicates the optimized excited state in gas phase; *b* indicates the optimized excited state in solution.

## *D*. Schematic diagram PyCz/PS porous nanofibers towards the target explosives

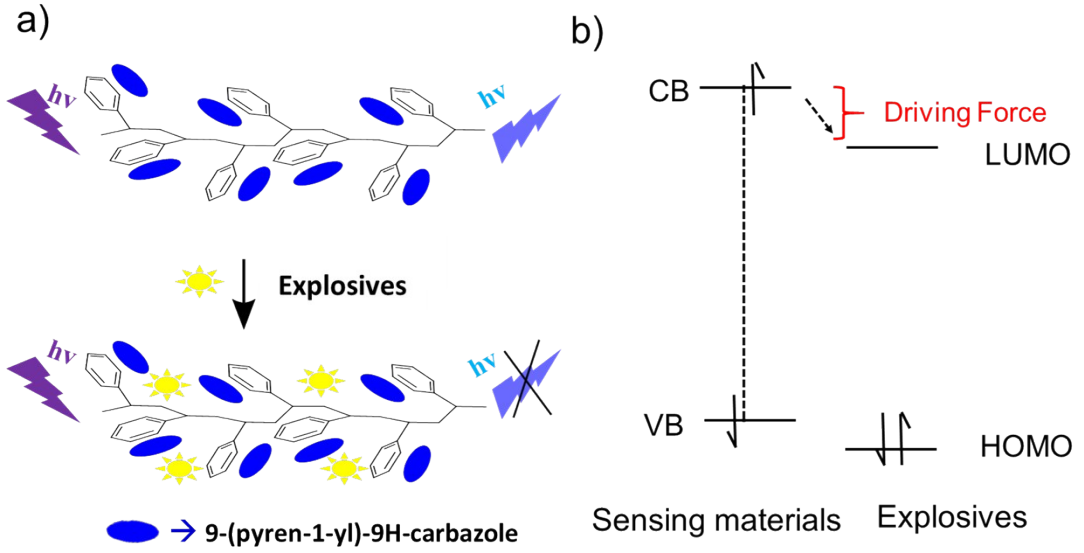


**Fig. S3** (a) Schematic molecular stacking modes and quenching process of PS/PyCz porous electrospun nanofibers. (b) Photo-induced electron transfer mechanism of the sensing materials on the detection of nitro explosives.

## *E*. Time-dependent fluorescence quenching process of PS/PyCz nanofibrous film in perfume

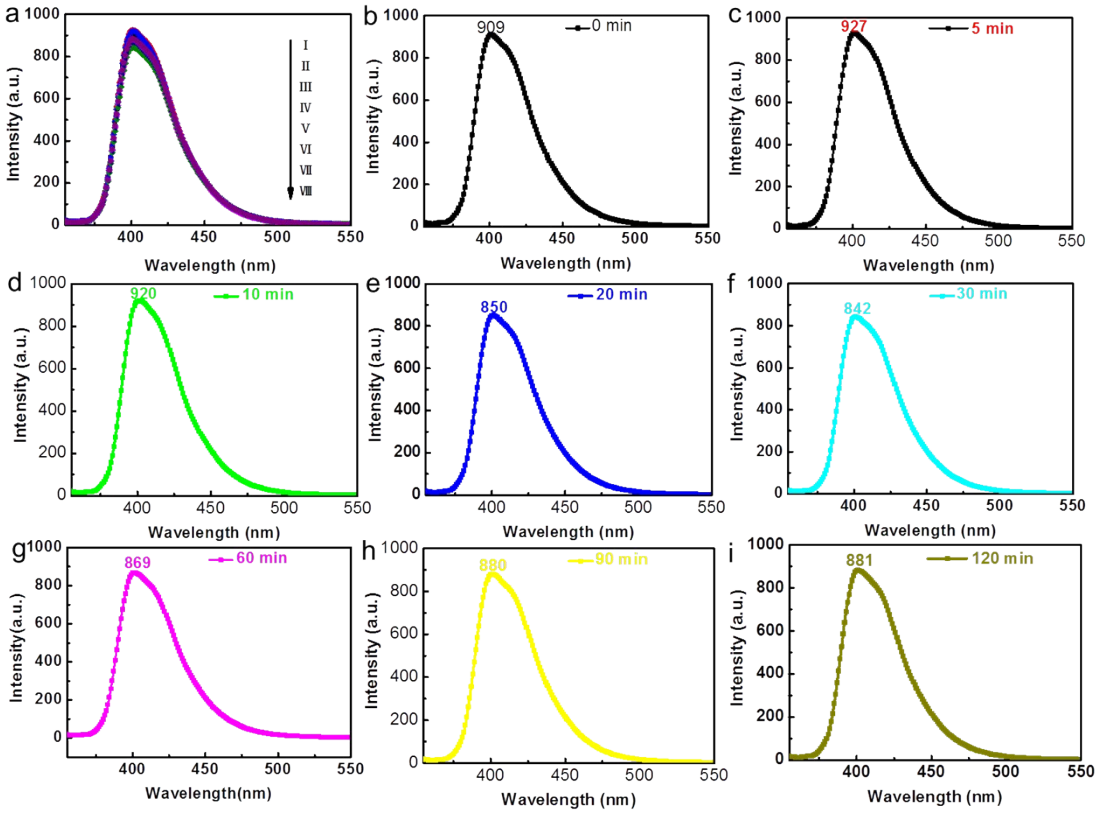


**Fig. S4** Detailed time-dependent fluorescence quenching process of PS/PyCz porous nanofibrous film towards perfume vapor ( Ⅰ to Ⅷ : 0, 5, 10, 20, 30, 60, 90, 120 min; $\lambda_{ex}$ = 340 nm).

## *F*. Fluorescent intensity changes for PS/PyCz porous nanofibrous film in wine, juice and scallion vapor

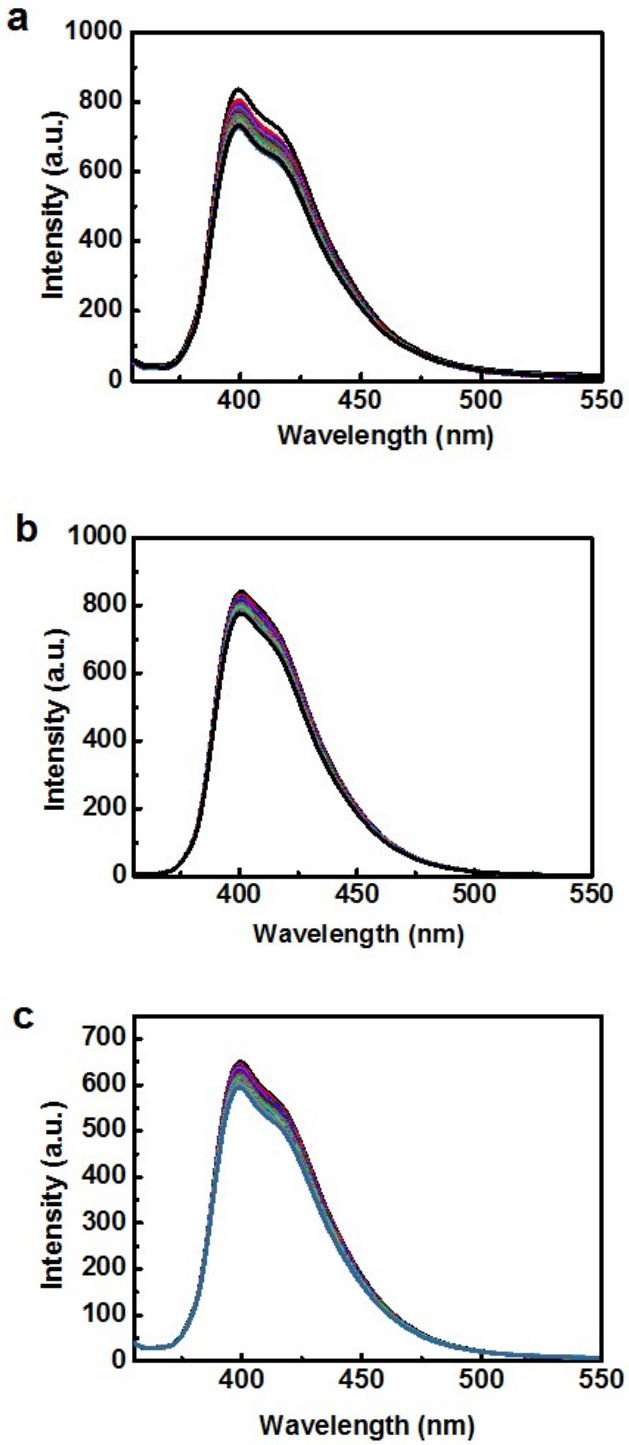


**Fig. S5** Time-dependent fluorescence quenching process of PS/PyCz porous nanofibrous film towards (a) juice vapor, (b) wine vapor and (c) scallion vapor in 2 h. The emission spectra were collected every 5 minutes.

## *G*. SEM image/FLM photograph of PEO/ PyCz hybrid fibers

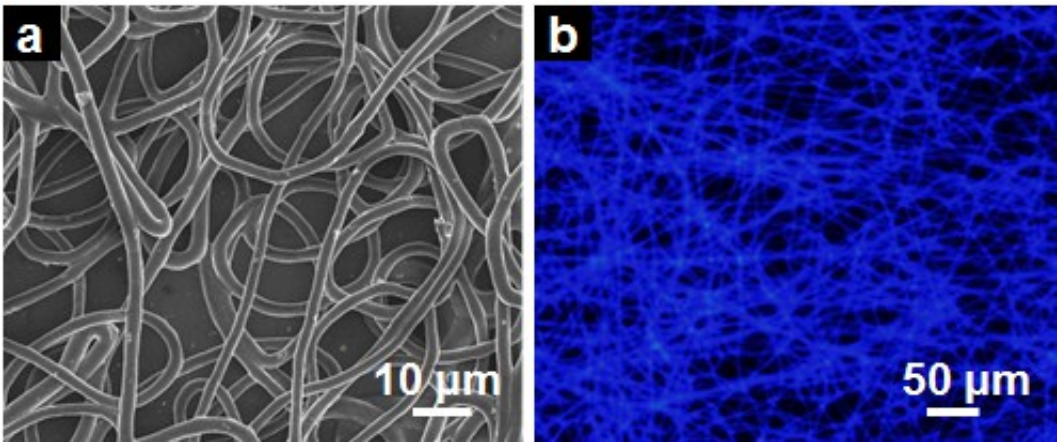


**Fig. S6** (a) SEM image and (b) FLM photograph of PEO/PyCz nanofibers.

## *H*. Excitation and emission spectra of PEO/PyCz nanofibers

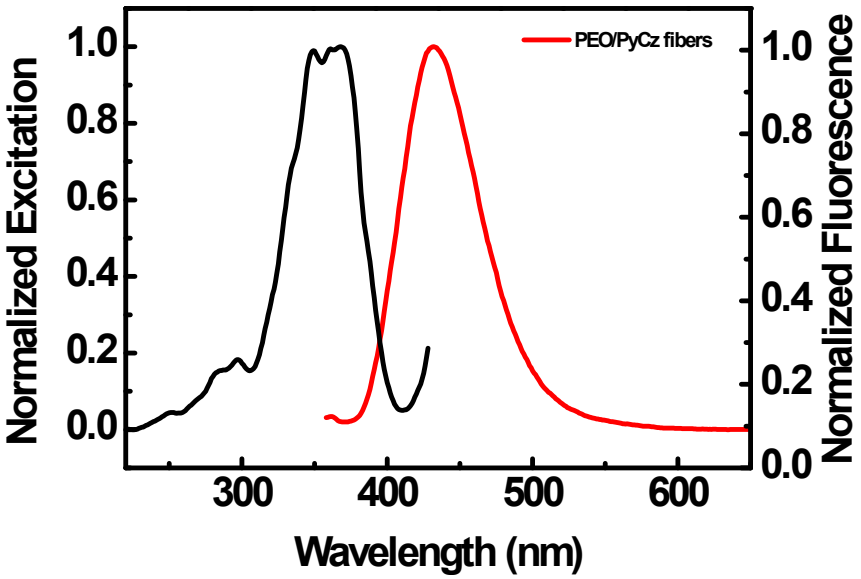


**Fig. S7** Excitation ($\lambda_{em}$ = 432 nm) and emission spectra ($\lambda_{ex}$ = 348 nm) of PEO/PyCz fibers.

## *I*. Fluorescent intensity for PEO/PyCz nanofibrous film in wine, juice and scallion vapor

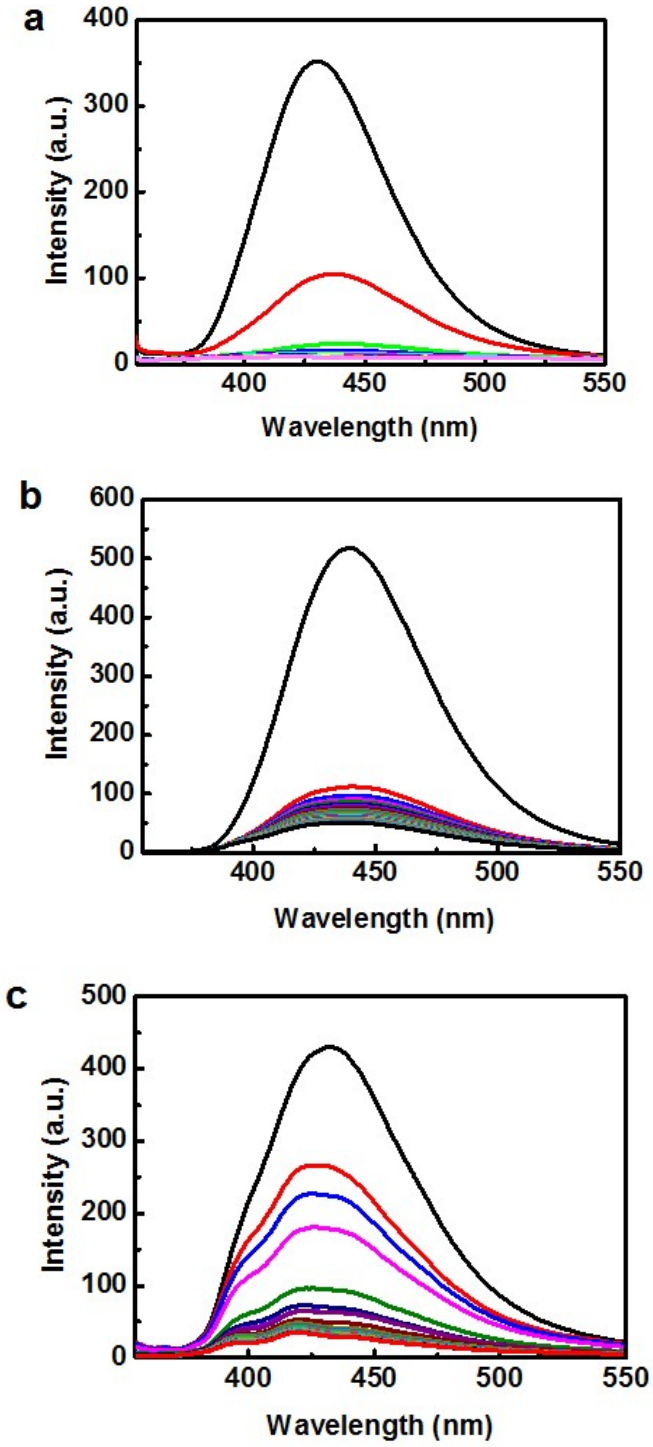


**Fig. S8** Time-dependent fluorescence quenching process of PEO/PyCz nanofibrous film towards (a) juice vapor, (b) wine vapor and (c) scallion vapor in 2 h.

## *J.* Time-dependent fluorescence quenching process of PEO/PyCz fibrous film under different humidity

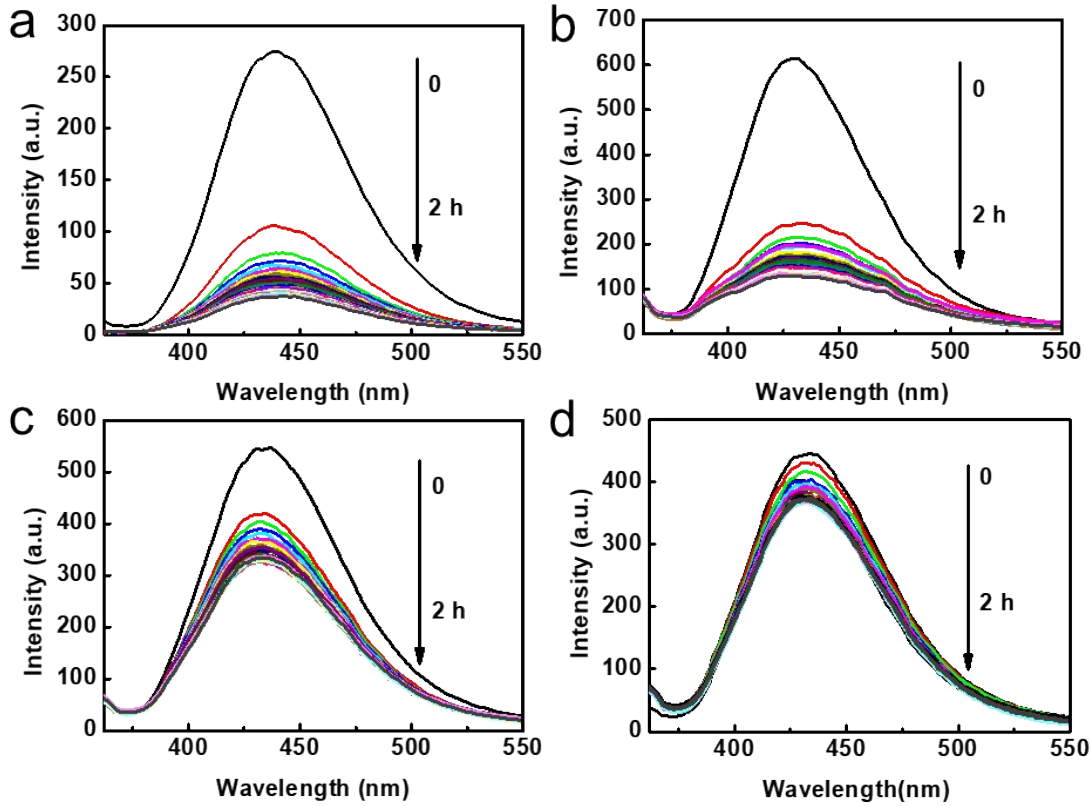


**Fig. S9** Time-dependent fluorescence quenching process of PEO/PyCz fibrous film towards different water amount degrees of (a) 0.5, (b) 0.3, (c) 0.2 and (d) 0.1 μL in a 3.5 mL quartz cell.

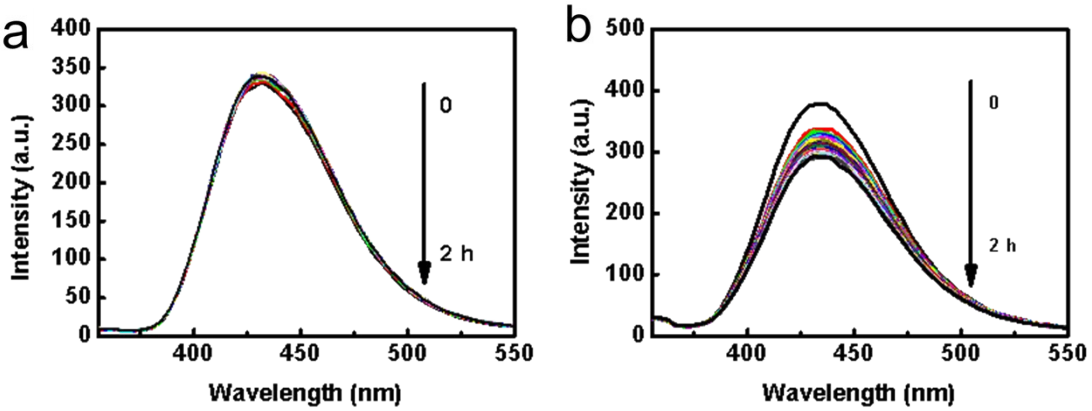


**Fig. S10** Time-dependent fluorescence quenching process of towards different amount degrees of (a) 0.1 μL and (b) 0.3 μL $Cu(NO_3)_2$ aqueous solution sealed in a 3.5 mL quartz cell.

## *K*. Fluorescence quenching efficiency of electrospun PS/PyCz porous film in NB vapor

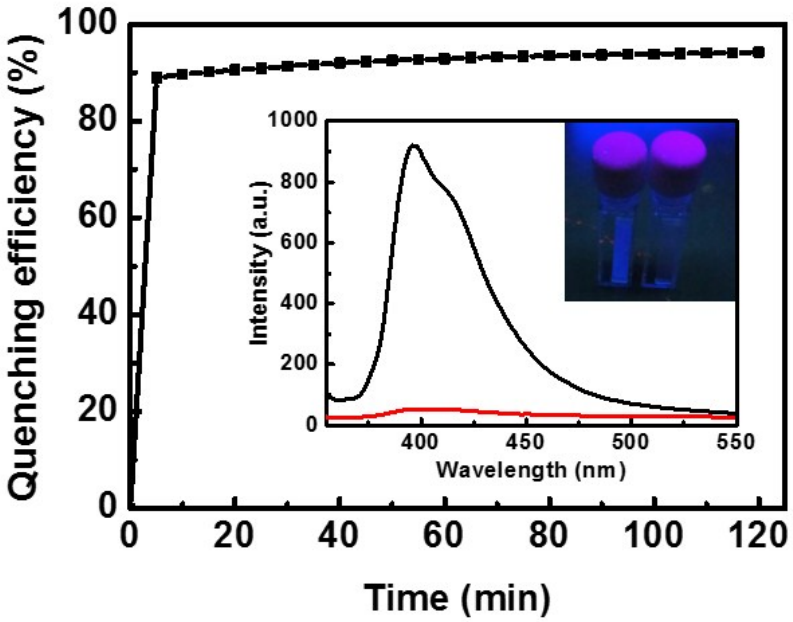


**Fig. S11** Fluorescence quenching efficiency of PS/PyCz film towards NB vapor for 2h.

## *L*. Energy levels of HOMO and LUMO orbitals of PyCz and the target explosives

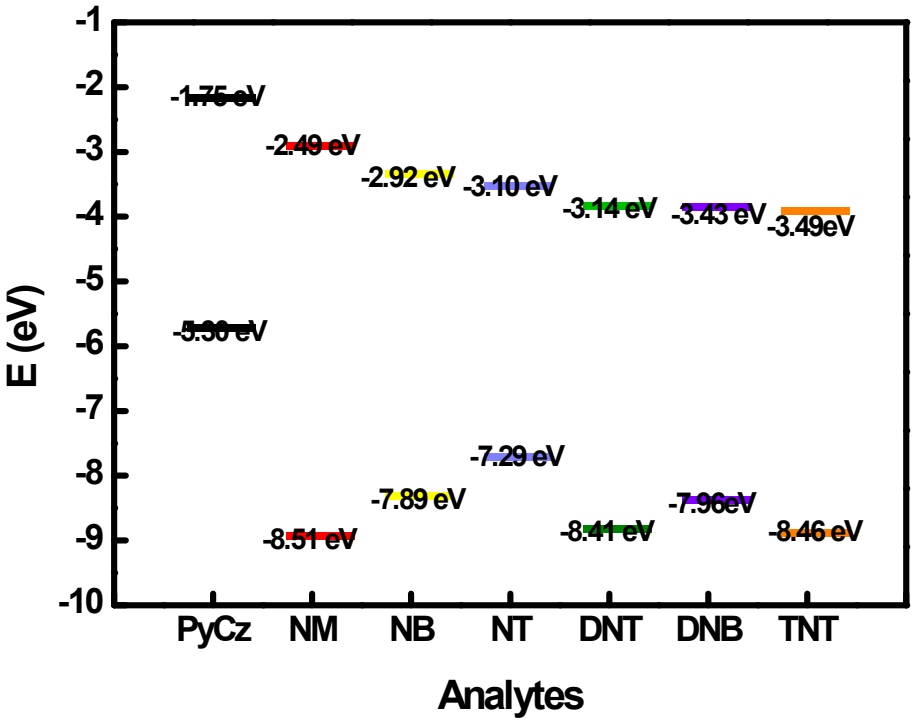


**Fig. S12** Energy levels of HOMO and LUMO orbitals of ground state PyCz and the target explosives. Geometry optimization and energy calculation were performed by density-functional theory with a basis of B3LYP/6-31G(d).

## *M*. Fluorescence quenching results

**Table S2.** Summary of fluorescence quenching efficiencies of PS/PyCz porous nanofibrous films and PEO/PyCz nanofibrous films towards the various analytes.

| | NM | NB | NT | DNT | DNB | TNT |
|---|---|---|---|---|---|---|
| PS/PyCz | 0.92 | 0.95 | 0.88 | 0.77 | 0.74 | 0.45 |
| PEO/PyCz | 0.90 | 0.92 | 0.79 | 0.65 | 0.60 | 0.89 |

| | Urea | Naphthalene | Smoke | Water | Perfume | Juice | Wine |
|---|---|---|---|---|---|---|---|
| PS/PyCz | 0.04 | 0.05 | 0.08 | 0.05 | 0.10 | 0.04 | 0.06 |
| PEO/PyCz | 0.04 | 0.03 | 0.09 | 0.94 | 0.76 | 0.96 | 0.90 |

## *N*. Supporting data for the quenching mechanism on the detection of trace water

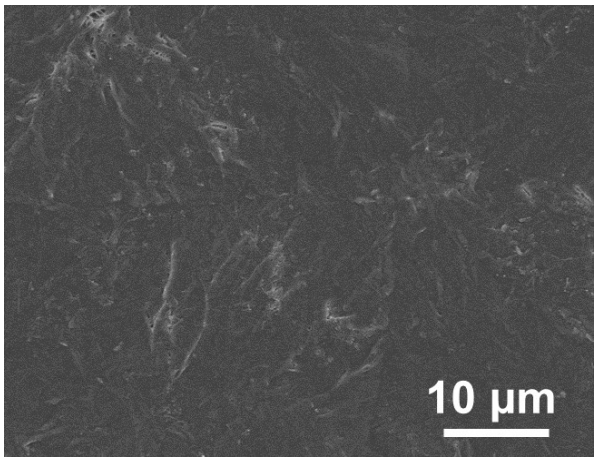


**Fig. S13** SEM image of PEO/PyCz electrospun nanofibers after exposure to water vapor for 2 h.

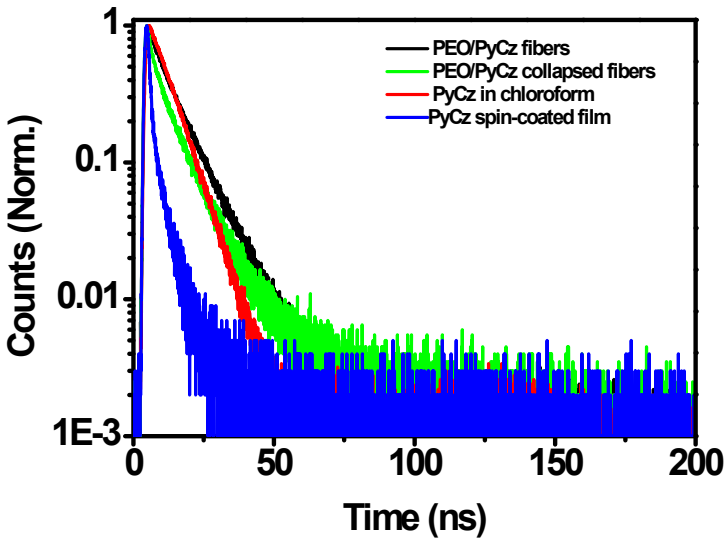


**Fig. S14** Fluorescence decay profiles of PEO/PyCz original nanofibers, collapsed nanofibers, PyCz chloroform solution and spin-coated film.

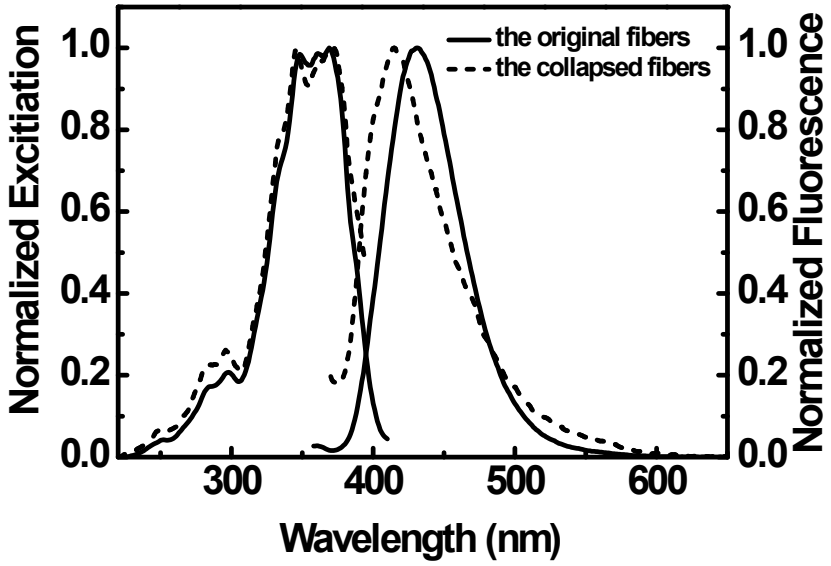


**Fig. S15** The excitation and emission spectra of PEO/PyCz electrospun nanofibers (a) before and (b) after exposure to water vapor for 2 h.

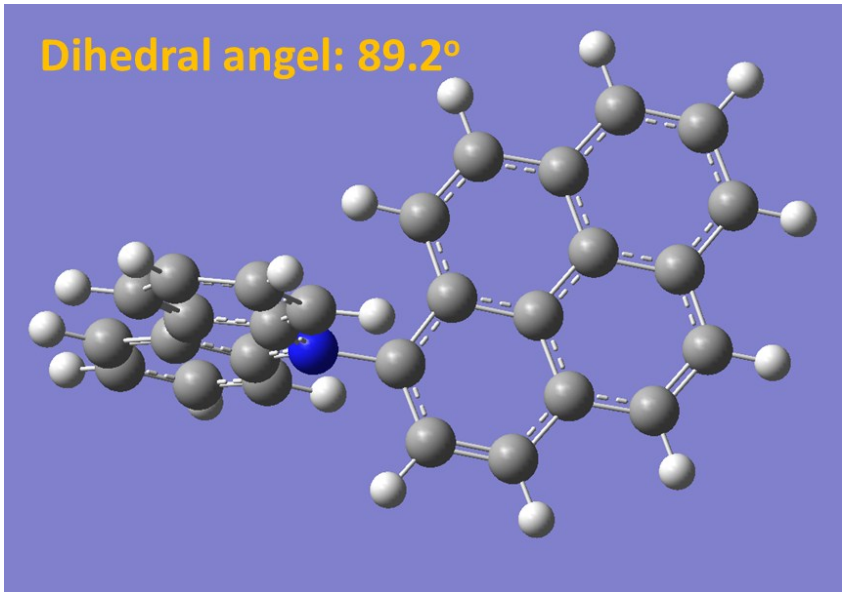


**Fig. S16** The optimized geometry structure of excited state of PyCz. The dihedral angle of the carbazole and pyrene units is 89.2°.

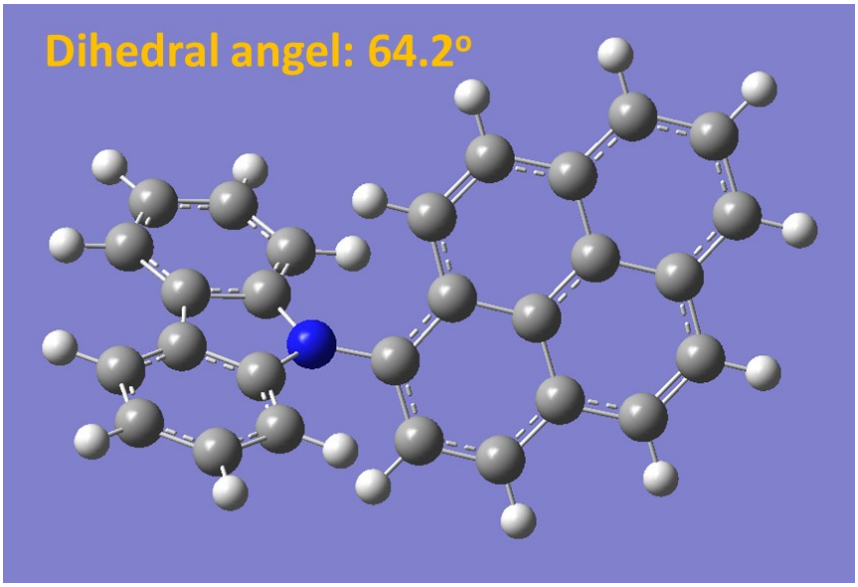


**Fig. S17** The optimized geometry structure of excited state of PyCz in chloroform solution. The dihedral angle of the carbazole and pyrene units is 64.2°.

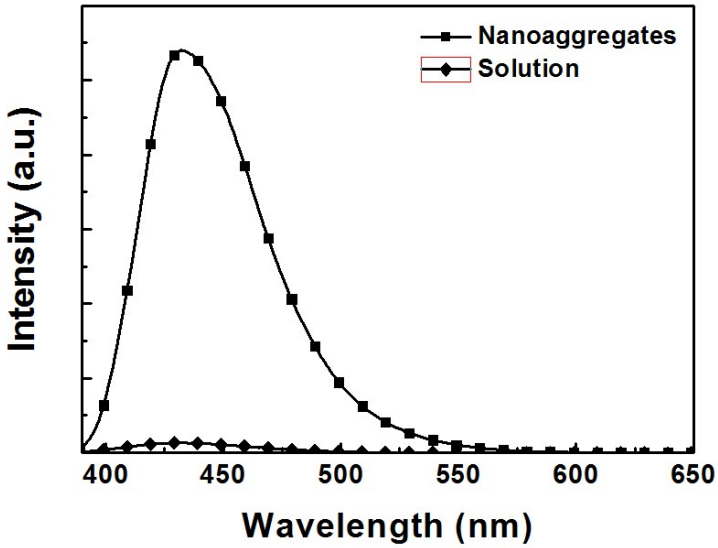


**Fig. S18** Fluorescence spectra of PyCz acetone solution (0.3 mM) and nanoaggregates in acetone:water (v:v=1:11) mixed solution (PyCz:0.3 mM). Notes: The nanostructures are prepared as follows. A certain amount of acetone solution of PyCz (3 mM, 0.5 mL) was injected dropwise into 5 mL water and stirred for 3 min at 25 °C.

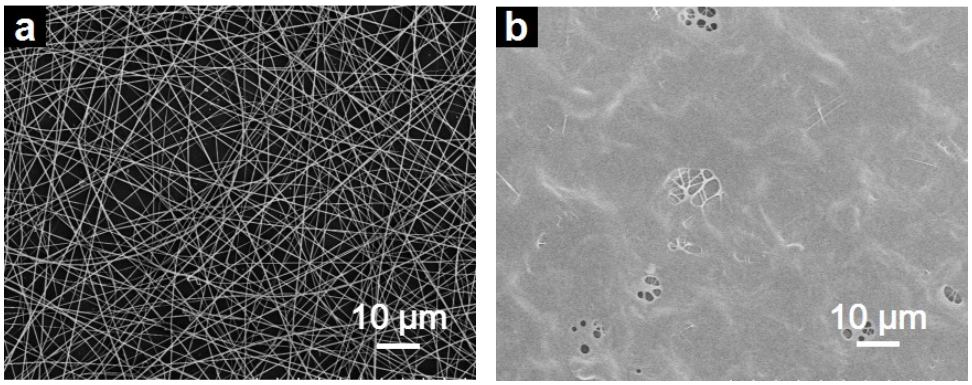


**Fig. S19** FESEM images of (a) the obtained electrospun PNIPAM/PyCz nanofibrous membrane in air and (d) the PNIPAM/PyCz membrane exposed to water vapor for 2 h.

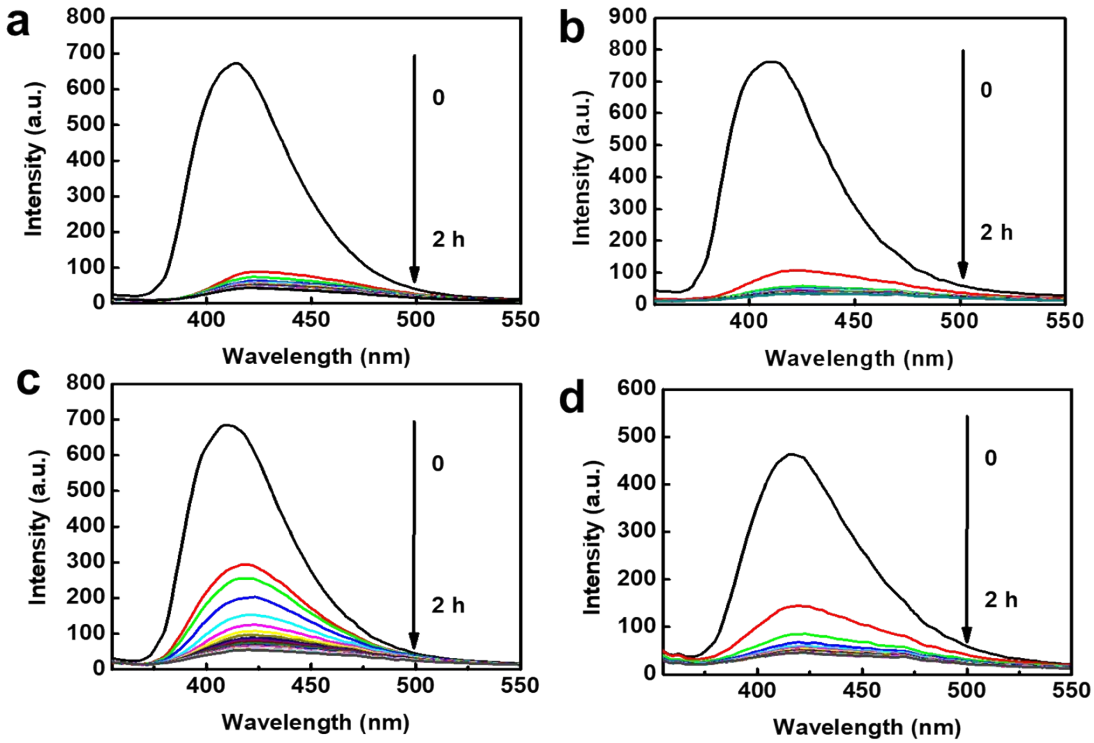


**Fig. S20** Time-dependent fluorescence quenching process of PNIPAM/PyCz nanofibers towards water (a), juice (b), wine (c) and scallion (d) in vapor for 2 h.